Supplementary Information

Nanomaterial-induced modulation of hormonal pathways enhances plant cell growth

Zhenyu Wang,[a,b,c] Junfeng Tang,[a] Liqi Zhu,[a] Yan Feng,[a] Le Yue,[a,b,c] Chuanxi Wang,[a,b,c] Zhenggao Xiao,[a,b,c] Feiran Chen, *[a,b,c]

[a] Institute of Environmental Processes and Pollution Control, and School of Environmental and Civil Engineering, Jiangnan University, Wuxi 214122, China

[b] Jiangsu Engineering Laboratory for Biomass Energy and Carbon Reduction Technology, Jiangnan University, Wuxi 214122, China

[c] Jiangsu Key Laboratory of Anaerobic Biotechnology, Jiangnan University, Wuxi 214122, China

*Corresponding author. E-mail address: chenfeiran@jiangnan.edu.cn (Dr. Feiran Chen).

Number of pages: 13

Number of figures: 14

Number of texts: 3

Number of tables: 3

List of Supplementary Information

Figure S13. Sparse partial least-squares discriminate analysis (sPLS-DA) score plots of metabolites in BY-2 cells from control and NMs exposure ($nMnFe_2O_4$, or N-CDs), and sPLS-DA plot of data from $nMnFe_2O_4$ and N-CDs exposure.

Figure S14. Abundance of typical metabolites altered by $nMnFe_2O_4$ and N-CDs.

Text S1. ICP-MS measurement for $nMnFe_2O_4$ and contents of K, P, Cu, Fe, Mn, Ca, and Zn.

Text S2. Magnetization measurement of BY-2 cells.

Text S3. LC-MS/MS analysis of metabolites.

Table S1. The hydrodynamic diameter and zeta potential of NMs.

Table S2. Sensitivity, detection limits and R^2 for multi-element detection by ICP-MS.

Table S3. Primers used for qRT-PCR.

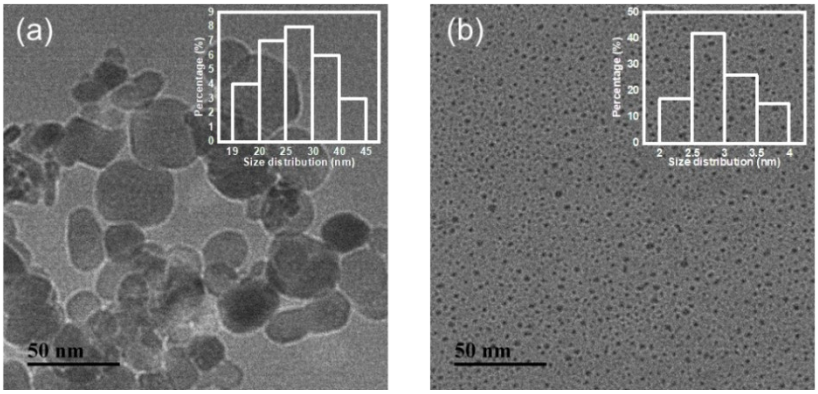

Figure S1. TEM images of $nMnFe_2O_4$ (a) and N-CDs (b).

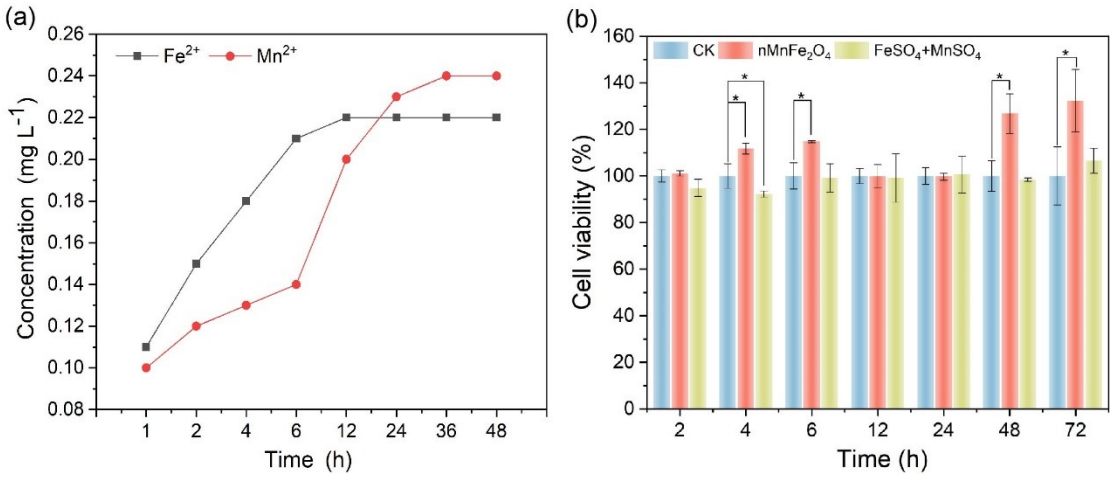

Figure S2. Dissolution of $nMnFe_2O_4$ in 1/2 MS medium (a), and viability of cells exposed to 1 mg L^{-1} $nMnFe_2O_4$ or $FeSO_4 \cdot 7H_2O$+$MnSO_4 \cdot H_2O$ at dose equivalent to that of ions released from $nMnFe_2O_4$ (b). For a given exposure time, the significant differences between control and different treatments are marked with asterisks (n=3).

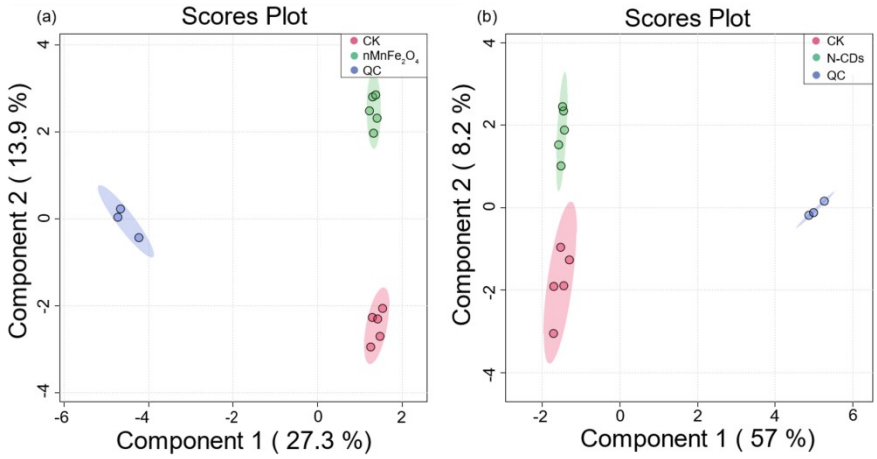

Figure S3. Sparse partial least-squares discriminate analysis (sPLS-DA) score plots of data from control sample, $nMnFe_2O_4$ (a) or N-CDs (b)-exposed sample, and QC sample.

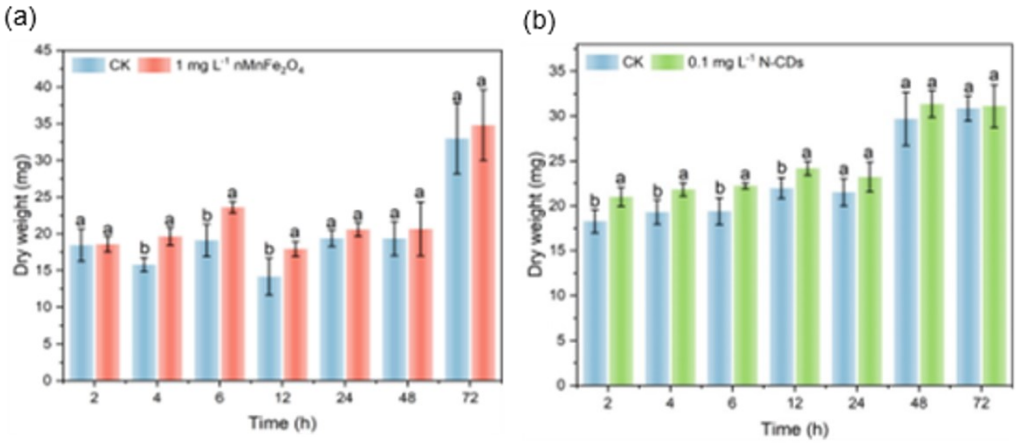

Figure S4. The dry weight of BY-2 cells exposed to $nMnFe_2O_4$ (a) or N-CDs (b), respectively. For a given exposure time, the significant difference between control and NMs treatment is marked with lowercase letters (n=3).

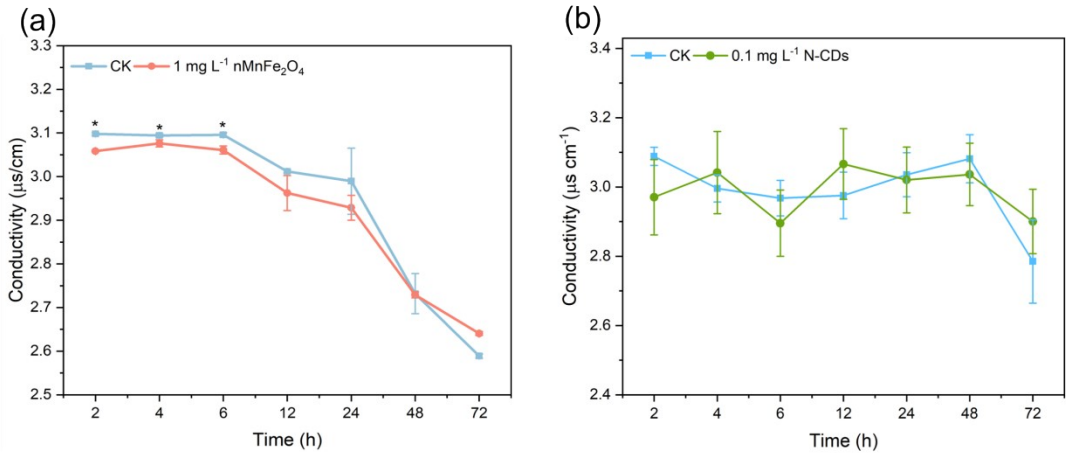

Figure S5. The conductivity of cell culture medium spiked with 1 mg L^{-1} $nMnFe_2O_4$ (a) and 0.1 mg L^{-1} N-CDs (b). For a given exposure time, the significant difference between control and NMs treatment is marked with an asterisk (n=3).

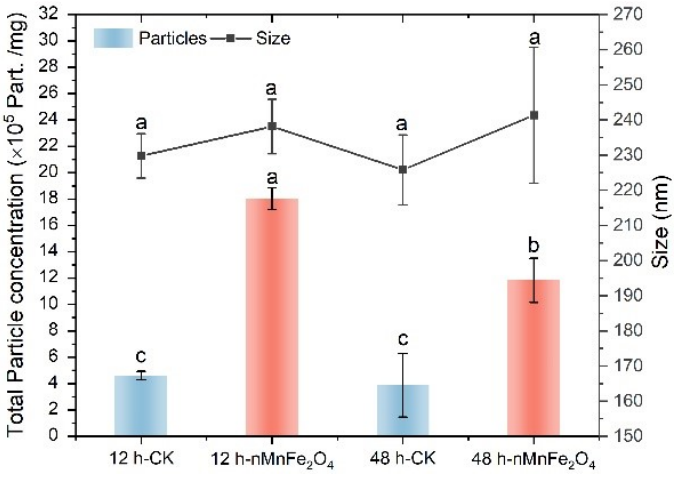

Figure S6. The particle size distribution and particle concentration of $nMnFe_2O_4$ in BY-2 cells under exposure for 12 h and 48 h. The significant difference between control and $nMnFe_2O_4$ treatment is marked with lowercase letters (n=3).

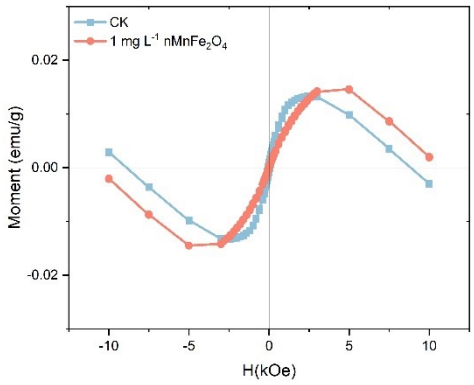

Figure S7. The VSM of BY-2 cells exposed to $nMnFe_2O_4$ for 12 h.

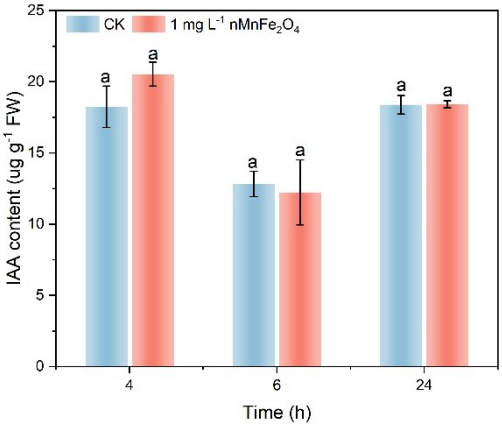

Figure S8. The IAA content in BY-2 cells from the control and $nMnFe_2O_4$ treatment. The significant difference between control and $nMnFe_2O_4$ treatment is marked with

lowercase letters (n=6).

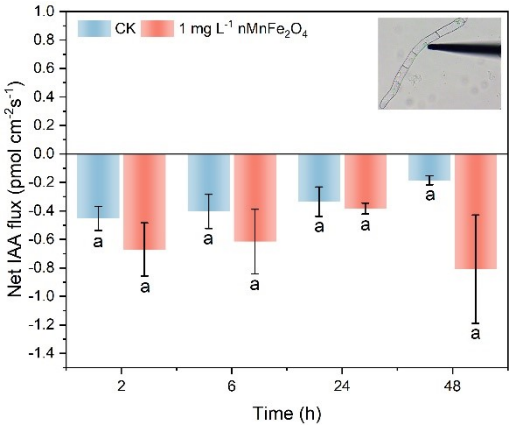

Figure S9. The net IAA flux in BY-2 cells exposed to $nMnFe_2O_4$. The significant difference between control and $nMnFe_2O_4$ treatment is marked with lowercase letters (n=6).

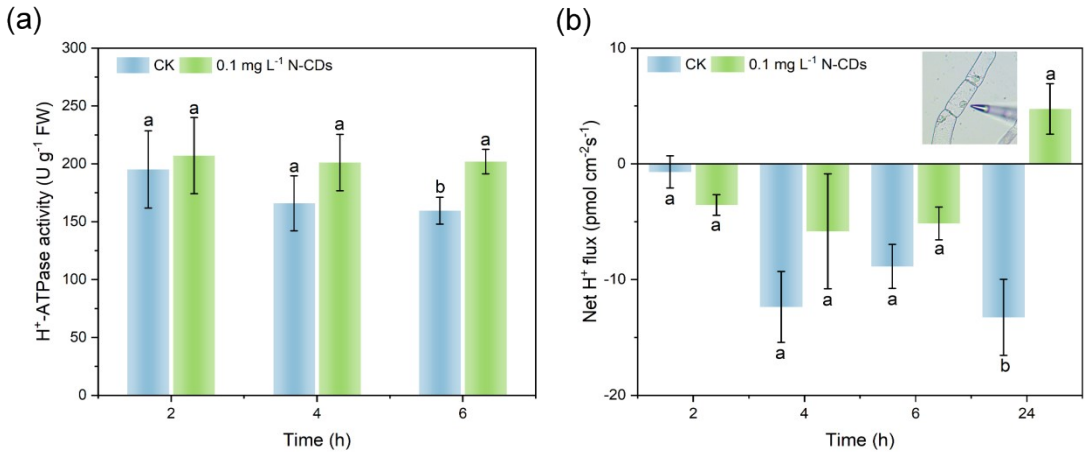

Figure S10. The H^+-ATPase activity (a) and the net H^+ flux (b) in BY-2 cells after N-CDs exposure. The significant difference between control and $nMnFe_2O_4$ treatment is marked with lowercase letters (n=3 for H^+-ATPase and n=6 for H^+ flux).

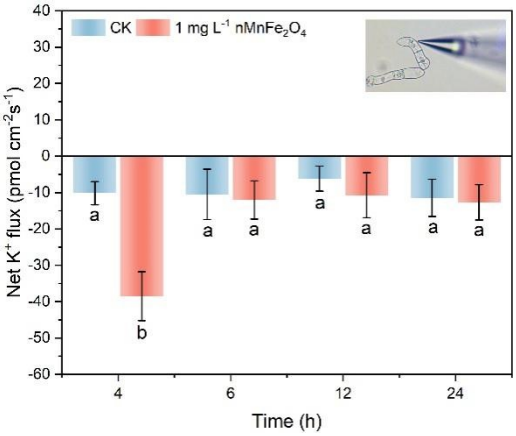

Figure S11. The net K^+ flux in BY-2 cells after $nMnFe_2O_4$ exposure. The significant difference between control and $nMnFe_2O_4$ treatment is marked with lowercase letters (n=6).

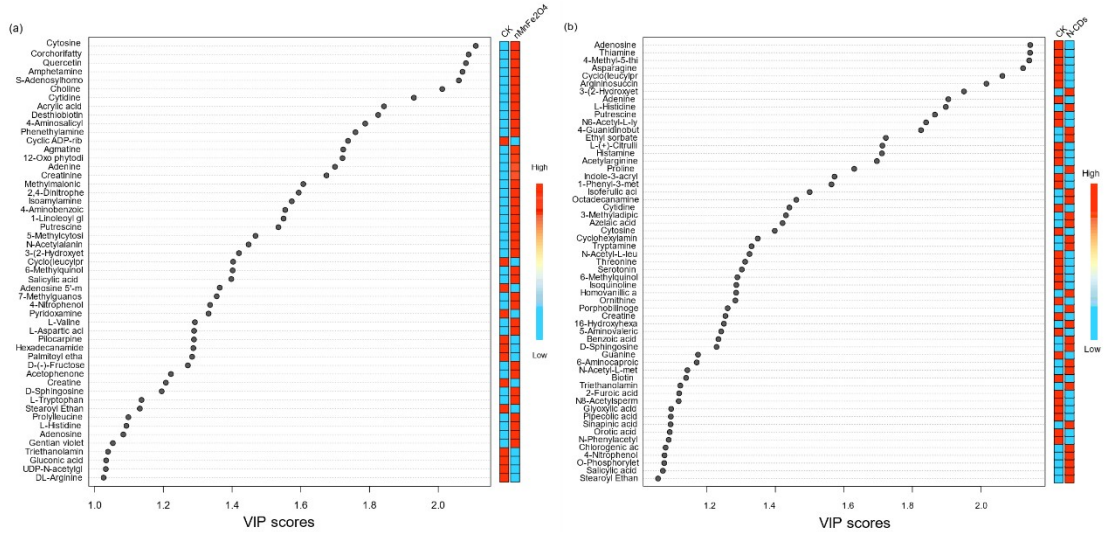

Figure S12. Variable important in projection (VIP) scores from sparse partial least-squares discriminate analysis (sPLS-DA) showing the discriminating metabolites altered by $nMnFe_2O_4$ (a) and N-CDs (b). Red and blue scale bar represented the up-and down-regulation of metabolites.

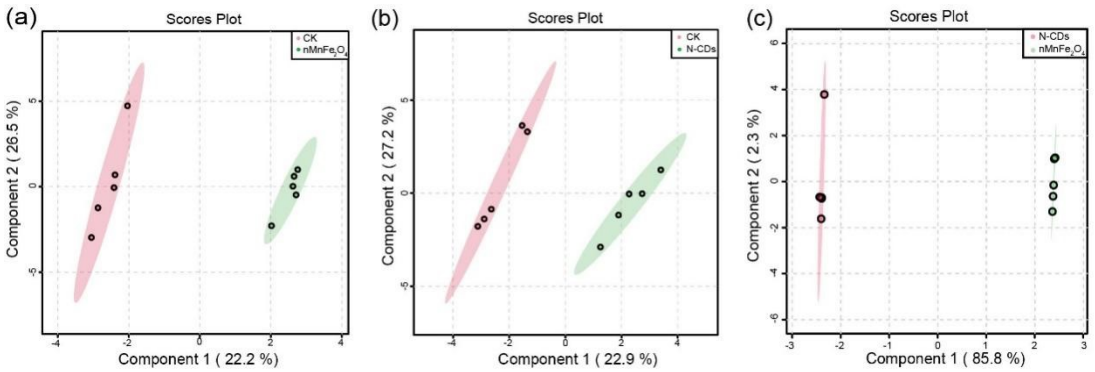

Figure S13. Sparse partial least-squares discriminate analysis (sPLS-DA) score plots of metabolites in BY-2 cells from control and NMs exposure ($nMnFe_2O_4$ (a), N-CDs (b)), and sPLS-DA plot of data from $nMnFe_2O_4$ and N-CDs exposure (c).

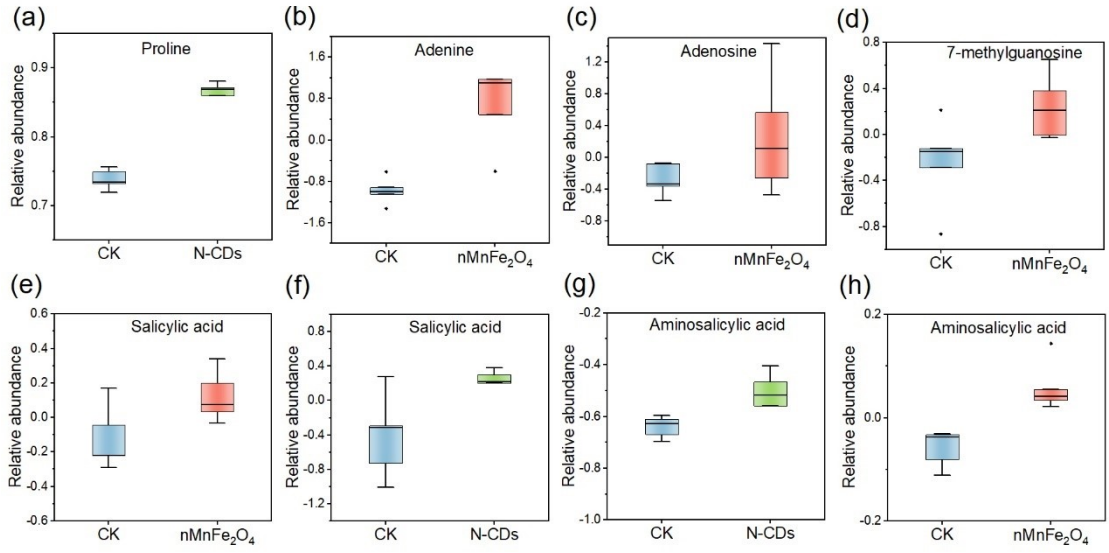

Figure S14. Abundance of typical metabolites altered by $nMnFe_2O_4$ and N-CDs.

Text S1. ICP-MS measurement for $nMnFe_2O_4$ and contents of K, P, Cu, Fe, Mn, Ca, and Zn

The particle size distribution and particle concentration of $nMnFe_2O_4$ in BY-2 cells exposed with 1 mg mL^{-1} were measured by single particle inductively coupled plasma-mass spectrometry (sp-ICP-MS). 100 mg cells were collected after washing thrice with PBS and mixed with 4 mL MES buffer (20 mM, pH 5.0). Later, cell samples were fully vortexed, further sonicated. Enzyme digestion was performed by adding 1 mL

Macerozyme R-10 enzyme solution (20 mg mL^{-1}) and incubating on a shaker (37℃, 200 rpm) for 24 h. After digestion, the samples were settled for 1 h and centrifugated to obtain the supernatant. The supernatant was filtered with 0.22 μm membrane and diluted 10 times with Mill-Q water for preparation of sp-ICP-MS (Thermo Scientific™ iCAP™ TQ ICP-MS, Germany).

The contents of K, P, Cu, Fe, Mn, Ca, and Zn in BY-2 cells was measured by inductively coupled plasma mass spectrometer (ICP-MS, Thermo Scientific™ iCAP™ TQ ICP-MS, Germany). Microwave-assisted acid digestion (CEM corp, Matthews. NC) of dried BY-2 cells (25 mg) was carried out with 3 mL Mill-Q water and 3 mL guaranteed reagent HNO_3. After acid digestion, the acid solution was filtered with 0.22 μm membrane and diluted two times for ICP-MS analysis. To evaluate the accuracy of the method, a standard reference material (bush branches and leaves, GBW07602) was measured with the same procedure (Table S2). For quality control, the multi-element standard solution was measured every ten samples.

Text S2. Magnetization measurement of BY-2 cells.

To determine the uptake of $nMnFe_2O_4$ by BY-2 cells, the magnetization of the cells was quantified with a vibrating sample magnetometer (VSM) LakeShore7404 with a detection limit of ~0.5μemu. Cells from control and 1 mg mL^{-1} $nMnFe_2O_4$ exposure for 12 h and 48 h were collected and washed thrice with PBS (pH = 7.2), freeze-dried for 24 h and ground to powder. Approximately 10 mg fine powder of the freeze-dried cells was analyzed by VSM at room temperature within ± 3T magnetic fields. Before measurement, the calibration of instrument was conducted with pure nickel sphere reference sample at 10 kOe.[1]

Text S3. LC-MS/MS analysis of metabolites.

The mobile phase A (H_2O, 0.1% formic) and B (acetonitrile, 0.1% formic acid) were used for elution of the Acquity HSS T3 column (2.1 × 100 mm, 1.8 μm) which was applied for rapid separation of analytes. The elution gradient was as follows: 0 min 5% B; 1.5 min 5% B; 15.5 min 100% B; 16 min 5% B; 18 min 5% B. Besides, an Agilent Hilic Poroshell 120 column (2.1 × 100 mm, 2.7 μm) was used together with mobile phase A (H_2O, 0.1% formic, 5 mM ammonium acetate) and mobile phase B (95% acetonitrile, 0.05% formic acid, 5 mM ammonium acetate). The elution gradient was as follows: 0 min 98% B; 7 min 75% B; 10 min 10% B; 13 min 10% B; 13.5 min 98% B; 15 min 98% B. The injection volume and the flow rate were 5 μL and 0.35 mL min^{-1}, respectively. The QC samples were used to evaluate the stability of the analytical system. The conditions of ESI were: sheath gas pressure, 35 arbitrary units; aux. gas flow, 15 arbitrary units; sweep gas flow, 0 arbitrary units; capillary temperature, 320 °C; aux. gas heater temperature, 350 °C. Spray voltage was 3.5 kV for ESI (pos) and −3.0 kV for ESI (neg). Compound Discoverer 3.1 software (Thermo Fisher Scientific, USA) coupled with the mzCloud and ChemSpider libraries were used to process the raw date. A supervised partial least-squares discriminant analysis (PLS-DA) clustering method was applied via online resources (http://www.metaboanalyst.ca/). The pooled QC sample was measured every eight samples. To thoroughly examine the QC data, the variations in peak areas were calculated (the relative standard deviation, RSD), and a cut-off criterion (of 30% RSD) was applied.[2] The low variations of QC data and the clear separation of QC data with those from control and NMs-exposed samples (Fig. S3) demonstrated the reproductivity, stability, and accuracy of analytical runs. The

differential metabolites were determined by the variable importance in projection (VIP) score which rank the metabolites based on their importance to the entire model. Metabolites with VIP score > 1 or t-test p value < 0.05 were regarded as statistically significant.

Table S1. The hydrodynamic diameter and zeta potential of NMs.

NMs		Hydrodynamic diameter(nm)	Zeta potential(mV)
$nMnFe_2O_4$	DI water	161.04 ± 4.27	-11.27 ± 0.61
	1/2 MS	430.13 ± 16.55	-22.86 ± 0.78
N-CDs	DI water	136.07±4.06	-6.48±0.06
	1/2 MS	353.33±2.81	-10.77±0.21

Table S2. Sensitivity, detection limits and R^2 for multi-element detection by ICP-MS.

Elements	Linearity range (mg/L)/R^2	Linearity equation	Detection limit (ng/L)	Bush branches and leaves (GBW07602) Standard value (μg/g)	Bush branches and leaves (GBW07602) ICP-MS measured value (μg/g, n = 3)
Fe	0-10/0.9998	y = 82.795x – 50.180	329	1020 ± 67	1052 ± 37
Mn	0-0.1/0.9998	y = 1463.256x –64.847	36	58 ± 6	62 ± 1.20
Mg	0-10/0.9999	y = 198.958x –244.597	72	2870 ± 180	2825 ± 106
P	0-10/0.9999	y = 688.790x –1797.900	41	830 ± 40	774 ± 20
S	0-10/0.9999	y = 1097.677x –13716.033	895	3200 ± 300	3659 ± 29
K	0-10/0.9998	y = 81.791x – 3290.177	7832	8500 ± 500	8482 ± 194
Ca	0-10/0.9999	y = 5.7084x – 267.093	15612	22200 ± 1300	25742 ± 633
Zn	0-0.1/0.9981	y = 784.0974x –1170.635	21	20.6 ± 2.2	18 ± 2.76

Cu	0-0.1/0.9989	y = 6980.420x –792.382	29	5.2 ± 0.5	5.8 ± 0.17

Table S3. Primers used for qRT-PCR.

Gene Name	FW-Primer	RW-Primer
EF1α	TCACATCAACATTGTGGTCATTGGC	TTGATCTGGTCAAGAGCCTCAAG
ARF	ATAGAGGAGTAGAAGATAGCCAAAACA	TGAAGGTAGAGGTAGCATAAGGAATAG
IAA9	GAGGAGGAGGGCCAGAGTAA	TGTACAACTGTCCACCGACG
EXP	GATAAGCAATGTAGGAGGGGCTGG	TATGTCTGCCCAAATTGCCAGTTC
CYCB	AGAGAGGCCGTTGATTGGAT	GAAAGACAGGACACAGCAGC

Reference:

1. H. Tombuloglu, G. Tombuloglu, Y. Slimani, I. Ercan, H. Sozeri and A. Baykal, Impact of manganese ferrite ($MnFe_2O_4$) nanoparticles on growth and magnetic character of barley (*Hordeum vulgare L.*), *Environ. Pollut.*, 2018, **243**, 872-881.
2. H. G. Gika, G. A. Theodoridis, M. Earll and I. D. Wilson, A QC approach to the determination of day-to-day reproducibility and robustness of LC–MS methods for global metabolite profiling in metabonomics/metabolomics, *Bioanalysis*, 2012, **4**, 2239-2247.